

Article

Comparison of the Spatial Wind Erosion Patterns of Erosion Risk Mapping and Quantitative Modeling in Eastern Austria

Simon Scheper^{1,2,*}, Thomas Weninger³, Barbara Kitzler², Lenka Lackóová⁴, Wim Cornelis⁵, Peter Strauss³
and Kerstin Michel²

- ¹ Dr. Simon Scheper—Research | Consulting | Teaching, Eickhorst 3, 29413 Dähre, Germany
² Federal Research and Training Centre for Forests, Natural Hazards and Landscape, Seckendorff-Gudent Weg 8, 1131 Vienna, Austria; barbara.kitzler@bfw.gv.at (B.K.); kerstin.michel@bfw.gv.at (K.M.)
³ Federal Agency for Water Management, Institute for Land and Water Management Research, Pollnbergstraße 1, 3252 Petzenkirchen, Austria; thomas.weninger@baw.at (T.W.); peter.strauss@baw.at (P.S.)
⁴ Department of Landscape Planning and Land Consolidation, Slovak University of Agriculture in Nitra, Hospodárska 7, 94976 Nitra, Slovakia; lenka.lackoova@uniag.sk
⁵ Department of Environment-UNESCO Chair on Eremology, Ghent University, Coupure Links 653, 9000 Ghent, Belgium; wim.cornelis@ugent.be
* Correspondence: simonscheper@simonscheper.com

Abstract: Various large-scale risk maps show that the eastern part of Austria, in particular the Pannonian Basin, is one of the regions in Europe most vulnerable to wind erosion. However, comprehensive assessments of the severity and the extent of wind erosion risk are still lacking for this region. This study aimed to prove the results of large-scale maps by developing high-resolution maps of wind erosion risk for the target area. For this, we applied a qualitative soil erosion assessment (DIN 19706) with lower data requirements and a more data-demanding revised wind erosion equation (RWEQ) within a GIS application to evaluate the process of assessing wind erosion risk. Both models defined similar risk areas, although the assignment of severity classes differed. Most agricultural fields in the study area were classified as not at risk to wind erosion (DIN 19706), whereas the mean annual soil loss rate modeled by RWEQ was $3.7 \text{ t ha}^{-1} \text{ yr}^{-1}$. August was the month with the highest modeled soil loss (average of $0.49 \text{ t ha}^{-1} \text{ month}^{-1}$), due to a low percentage of vegetation cover and a relatively high weather factor combining wind speed and soil moisture effects. Based on the results, DIN 19706 is suitable for a general classification of wind erosion-prone areas, while RWEQ can derive additional information such as seasonal distribution and soil loss rates besides the spatial extents of wind erosion.

Keywords: hazard; soil protection; windbreaks; field length; DIN 19706; revised wind erosion equation; seasonal wind erosion risk



Citation: Scheper, S.; Weninger, T.; Kitzler, B.; Lackóová, L.; Cornelis, W.; Strauss, P.; Michel, K. Comparison of the Spatial Wind Erosion Patterns of Erosion Risk Mapping and Quantitative Modeling in Eastern Austria. *Land* **2021**, *10*, 974. <https://doi.org/10.3390/land10090974>

Received: 24 August 2021

Accepted: 15 September 2021

Published: 16 September 2021

Publisher's Note: MDPI stays neutral with regard to jurisdictional claims in published maps and institutional affiliations.



Copyright: © 2021 by the authors. Licensee MDPI, Basel, Switzerland. This article is an open access article distributed under the terms and conditions of the Creative Commons Attribution (CC BY) license (<https://creativecommons.org/licenses/by/4.0/>).

1. Introduction

Soil provides many services beneficial for both humans and nature, e.g., working as food supplier, carbon sequester, climate regulator, filter for water and pollutants, and cultural heritage storage [1,2]. Therefore, for a long time, soil degradation is among the most severe environmental threats [3,4], causing the loss of agricultural supply and triggering many off-site effects such as sedimentation, eutrophication of water bodies, or loss of genetic stock and biodiversity [3]. One of the major soil degradation processes is soil erosion [5]. Although water erosion is more frequently recognized and observed, wind is the main driver of erosion processes in drylands, which make up approx. 40% of the global land surface [6]. However, erosion by wind is often not given the same attention as erosion by water, both in science and in land management [7]. For example, in a review of 1697 articles, Borrelli et al. [8] investigated the presence of different soil erosion types and their modeling approaches. Only 2.3% of these articles considered wind erosion compared

to the 94.6% that considered water erosion studies. Still, this literature review also noticed an increase in wind erosion modeling studies in recent years.

Wind erosion is the process of detachment, transport, and deposition of soil particles by wind forces. In principle, wind erosion is the result of two types of forces that work against each other: the aerodynamic forces of the wind to detach and transport the soil particle, and gravity and particle cohesion that try to resist against the aerodynamic force by keeping the soil particle on the spot [9]. Typically, wind speeds of at least 5.0 m s^{-1} at 2 m above ground level are needed to detach soil particles [10]. In principle, dry sandy soils are the most easily detachable due to their low cohesion forces and are thus the most endangered soils [9]. In addition, many other environmental factors play crucial roles in the wind erosion process: atmospheric conditions such as precipitation and temperature influence soil moisture; soil characteristics such as soil texture affect soil resistance to erosion; land-use patterns, e.g., bare surfaces as well as protective structures such as windbreaks and land-surface characteristics control parameters such as topography, moisture and surface roughness [11].

Several European maps of wind erosion show that the Eastern part of Austria, mainly the Pannonian Basin, is one of the most affected regions within the European Union [12–14]. The Pannonian Basin is an example of a region characterized by high agricultural productivity, soils formed on aeolian or fine fluvial sediments, high wind speeds in the geomorphological gap between the Alps and the Carpathians, and high settlement pressure between the growing cities of Vienna and Bratislava. In addition, its phytogeographical location on the border of Steppe zones presents a risk to loose the preconditions for productive agriculture. Wind erosion in Austria, especially in the broader surroundings of Vienna covering the Pannonian region, was already a significant concern in 1770 when the Austrian empress Maria Theresa enacted reforestation to combat soil transport by wind due to the existence of wandering dunes [15]. Since the 1950s, windbreaks have been planted in eastern Austria to reduce wind speeds and protect the soils against detachment [16]. Despite these known risks and the established measures against wind erosion, only a few wind erosion studies exist for Austria [16,17]. To our knowledge, no field measurements on wind erosion have been made in Austria. Only large-scale (European or global) modeling studies at a relatively coarse spatial resolution with a static temporal resolution are available so far, although increasing knowledge on a regional scale is strongly needed to estimate future risks for agriculture. The link to regional studies is rarely seen, and an attempt is presented in this study.

According to the relevant literature on soil erosion modeling [8], the most applied models for assessing wind erosion are the empirical Wind Erosion Equation (WEQ—[18]) and its revised version (RWEQ—[19]), the more process-oriented single-event Wind Erosion Evaluation Program (SWEEP—[20]), and the Wind Erosion Prediction System (WEPS—[21]). Such models generally enable the quantification of soil loss rates as well as defining risk zones. However, they demand a high data input to make them applicable [22]. An alternative to high data demanding models are simplified risk maps based on evaluation schemes such as SoLoWind (Soil Loss by Wind Erosion, [23]) for Saxony, Germany, expert rule assessments for France [24] and Australia [25,26], potential wind erosion susceptibility maps in the Czech Republic [27] or Hungary [28], or the Index of Land Susceptibility to Wind Erosion (ILSWE) for Europe [13]. A frequently applied risk map approach for wind erosion is the German DIN 19706 ‘Soil quality—Determination of the soil exposure risk from wind erosion’ [29], which is primarily based on extensive wind erosion research of the Leibniz Centre for Agricultural Landscape Research (ZALF) [30–32]. DIN 19706 has already been applied on a national level for Germany [33] as it is also intended to be applied at different scales. Common to all these fewer data demanding approaches is the qualitative aspect that enables the classification of risk zones according to wind erosion by susceptibility/risk/hazard classes. As in empirical and physical-based models, qualitative assessments require several parameters to determine the area under risk. Such qualitative applications often sufficiently describe the needs of public authorities as they may easily im-

plement the results into their policy decisions, fulfilling the demands for good agricultural practices and serving as a tool for soil protection. Qualitative risk maps are also a suitable measure to raise awareness for soil erosion by wind. Furthermore, risk maps enable direct agricultural prevention measures such as tillage reduction or compensatory payments [34]. Still, the validity of such risk maps based on single model approaches is debatable as they are rather experience-based and often lack the documentation of scientific foundations such as physical relationships or extensive measurements. Relatedly, classification schemes of soil erosion maps are often expert-based and not transparently applied. A comparison and discussion of different scaling and categorization of soil erosion rates may facilitate selecting appropriate classification schemes.

Therefore, we aim to:

- (i) assess the spatial and temporal pattern of wind erosion risk for a selected study area in eastern Austria;
- (ii) discuss the validity of wind erosion assessment based on DIN 19706 and compare to the modeling results of RWEQ;
- (iii) discuss different classification schemes for soil erosion.

The present study focuses on the Austrian part of the Pannonian Basin. This region was selected due to its high potential for wind erosion resulting from its climatic and pedogenic characteristics and intensive agricultural land use.

2. Materials and Methods

2.1. Study Area

The study region covers 2319 km² in the province of Lower Austria, located in eastern Austria. It is part of the Pannonian Basin and is intersected by the river Danube. The elevation ranges from 133 m to 480 m with a mean of 182 m a.s.l. Slopes are flat to gently undulated (mean slope of 2.5 degrees) [35].

The long-term (1981–2010) mean temperature at the meteorological station Gross-Enzersdorf (see Figure 1) is 10.3 °C. The study region is within the driest regions in the country [36], with a long-term mean annual precipitation of 516 mm [37]. Additionally, mean wind speeds of 3.4 m s⁻¹ [37] are relatively high compared to other lowland regions in Austria. On average, 19 and 2 days per year are showing wind speeds above 6 Bft (≥ 11.3 m s⁻¹) and 8 Bft (≥ 17.5 m s⁻¹), respectively [37]. The main wind direction for the study region is northwest. A snow cover higher than 10 mm is present 31 days per year on average [37].

According to the digital Austrian soil map (eBod, [38]), soils in the study region are predominantly classified as chernozems, and there are also cambisols and fluvisols evolved from fine-grained sediments and loess. According to BFW [38], dominant topsoil textures are loam, loamy silt, and loamy sand (Figure 2). Most soils have organic carbon contents between 1.5% and 4.0% and inorganic carbon contents greater than 5.0%. The soil surveyors empirically rated the majority of agricultural fields with the highest productivity values [38].

The region is intensively cultivated, with 66% of the study area being used as agricultural land [39]. According to the field block data of 2020 [39], connected fields (so-called field blocks) without natural/artificial interruptions such as forests, streets, built-up areas, and streams have an average size of 9.5 ha. According to the latest agricultural statistics of 2016 [40] for the entire state of Lower Austria, approximately 44% of the states' agricultural area was used for winter crops (e.g., winter barley, winter oilseed rape), cover crops covered 22% of the area in winter, and 17% of arable land was ploughed in autumn and kept bare during winter. Most dominantly, fields were cultivated with grains, especially soft winter wheat (22% of the total arable land in 2020, [39]). A total of 3332 km of windbreaks (woody linear elements, width < 30 m) exist in the study region, with an average width of 14.5 m and an average height of 5.8 m, most of them planted by public authorities since the 1950s [16]. The mean field length in the main wind direction (315°), defined as natural field block, uninterrupted by different management, is 224 m with a maximum of 2832 m.

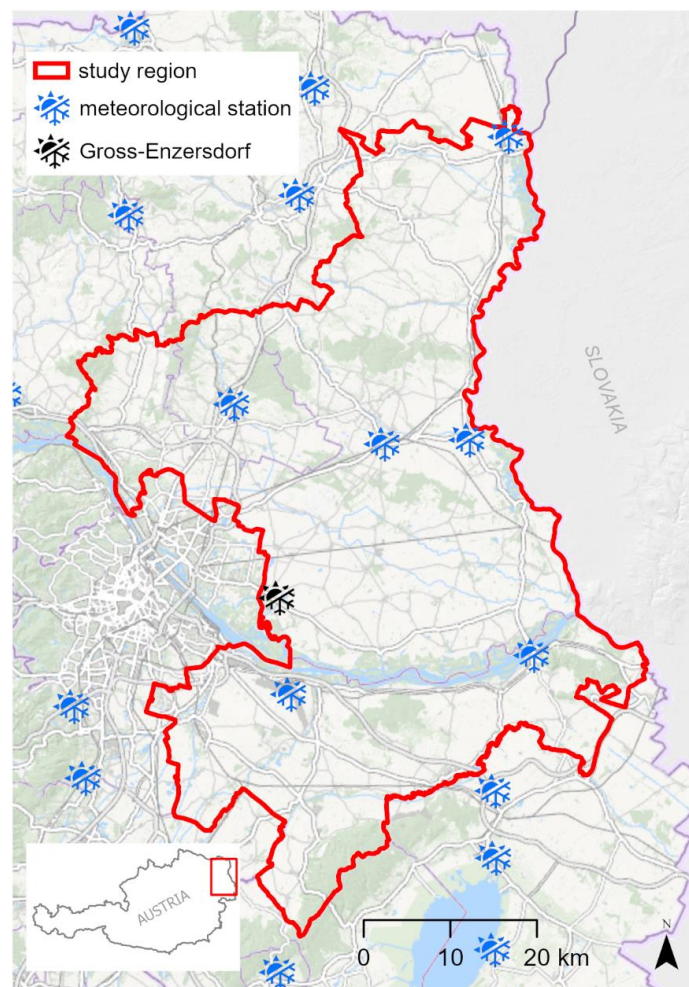


Figure 1. Location of the study region in Austria and meteorological stations used in this study. Gross-Enzersdorf is the meteorological station used for the general climatological description of the study region. For a complete list of meteorological stations, see Table S1.

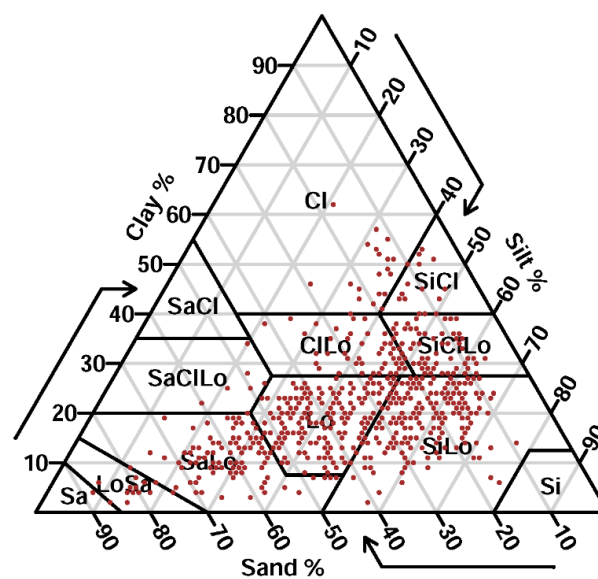


Figure 2. Soil texture diagram (USDA classification) of the topsoil in the study region ($n = 688$). Data are based on the digital soil map of Austria (eBod, [38]).

2.2. Datasets

We used primary (ready-to-use) and secondary (derivation of primary data) data sources to determine the mapping and modeling parameters. An overview of the datasets, including their resolution and sources, can be seen in Table 1. Meteorological measurements such as wind speed, wind direction, temperature, precipitation, relative humidity, pressure, and snow height were provided by the meteorological service of Austria (Zentralanstalt für Meteorologie und Geodynamik, ZAMG) for a total of 22 stations (seven within the study region, 15 in its surrounding; Figure 1, Table S1). The meteorological records cover eight years (2010–2017) in a daily resolution [41]. Rasterized long-term mean annual wind speeds (50 m height) were derived from a wind potential analysis by Krenn et al. [42]. Mean annual wind speeds were transformed to a height of 2 m using the logarithmic law [43]. Soil parameters were derived from the digital soil map (eBod) of Austria (1:25,000), which contains inter alia information about soil type, soil texture, and organic and inorganic carbon content [38]. Spatial information, extent, and cultivation data for field blocks at different years (2016–2020) were provided by Agrarmarkt Austria [39]. A total of 78 Sentinel-2 Level-2A satellite images (cloud cover $\leq 10\%$) were used to derive the vegetation cover at various stages from 2018 to 2020 [44]. Downloading and preprocessing of satellite imagery was done in R (v4.0.3; [45]) with the package *sen2r* [46]. Windbreaks are partly mapped by the public authority of Lower Austria. Missing windbreaks were manually digitalized using orthophotos from 2019 [47]. A digital surface model with a spatial resolution of 1 m was used to extract the mean heights of the windbreaks [48].

Table 1. Data description, resolution, and sources of datasets used for the mapping and modeling approach of wind erosion.

Data	Description	Data Type	Resolution (Spatial/Temporal)	Source
Meteorological measurements	Stational measurements at 22 stations, parameters: wind speeds, wind direction, temperature, precipitation, relative humidity, pressure, snow height	Point data	-/daily, 2010–2017	[41]
Mean annual wind speeds	Wind raster of Austria, 50 m height above ground level	Rasterized	100 m \times 100 m/-	[42]
eBod—digital soil map	Digital soil map of Austria with parameters such as soil type, soil texture, organic content, carbonates	Vectorized	1:25,000, based on soil profile/once	[38]
Field block	Field blocks 2015–2020, with cultivation data	Vectorized	1:2500/2015–2020	[39]
Sentinel-2 Level 2A	Multispectral satellite imagery	Rasterized	10 m \times 10 m/ 2018–2020	[44]
Windbreaks	Mapped windbreaks in Lower Austria	Vectorized	continuous mapping/ various years	Lower Austrian Authority for Land Reform
Orthophoto	Orthophoto of Austria	Rasterized	>0.15 m \times 0.15 m/ 2020	[47]
Digital surface model	Digital surface model based on laser scanning	Rasterized	1 m \times 1 m/-	[35]
Background information	Basemap, administrative borders	Rasterized, vectorized	various/various	[49,50]

2.3. Qualitative and Quantitative Erosion Modeling

The present study compares two different methods of evaluating soil erosion by wind: a qualitative and a quantitative assessment. Qualitatively evaluating soil loss by wind erosion, the German DIN 19706, was chosen as it is widely applied under mid-European conditions. To evaluate the soil loss of the study region quantitatively, we chose the RWEQ

due to its possibility to implement most of the regionally available data. Some of the datasets (e.g., digital soil map, parcels) could be used simultaneously for both approaches. As the nature of the approaches differs, our study allows evaluations of the different resulting spatial patterns rather than a direct comparison of single results such as risk classes or soil loss values. Additionally, the classification schemes for soil erosion risk and soil loss rates of the different approaches can be compared and discussed.

2.3.1. DIN 19706

The qualitative wind erosion evaluation scheme DIN 19706 is a matrix-based assessment that may be implemented in GIS environments. Adding additional factors such as wind speed, soil erodibility, types of fruits, crop rotation, and landscape elements (Figure S1) offers the possibility to improve the spatial representation [34]. The resulting wind erosion classes are ranked 0 (no susceptibility) to 5 (very high susceptibility).

The base of DIN 19706 forms the combination of a climate factor and a soil erodibility factor, resulting in the site-specific soil erosion susceptibility by wind. The climate factor considers mean annual wind speed at a height of 10 m above ground level. Wind speeds are categorized into six classes ($<2 \text{ m s}^{-1}$, $2\text{--}3 \text{ m s}^{-1}$, $>3\text{--}4 \text{ m s}^{-1}$, $>4\text{--}5 \text{ m s}^{-1}$, $>5\text{--}6 \text{ m s}^{-1}$, $>6 \text{ m s}^{-1}$). Rasterized mean annual wind speeds in the study region were reclassified following the proposed classes. These classes were merged with six soil erodibility classes based on soil texture and soil organic content (see Table S2 for the matrix). Among these classes, sandy soil and former peat soils were given the highest value of 5 (very high erodibility). Based on German textural classes, soil texture is determined by the composition of the fractions sand, silt, and clay, which are also components of the eBod. As the eBod only contains organic carbon content, the fraction was transformed to soil organic matter content by the van Bemmelen factor of 1.724 [51].

In the next step, the effects of crops and crop rotations were implemented, yielding the site and crop-specific soil erosion susceptibility by wind. Crops were ranked according to their soil surface cover in different periods of the year (closed vegetation cover in summer, early summer, spring, late fall, or perennial). However, DIN 19706 only proposes an assignment of the main types of fruits. As for our study region in eastern Austria, high differentiation of the type of fruits exists, and we used expert knowledge in combination with agricultural factsheets to determine typical cover of the not-listed fruits. A complete list of assignments can be found in the Supplement Material (Table S3). This process was realized on a field scale for the years 2018, 2019, and 2020. Crop rotation could not be considered because no comprehensive information was available for the whole study region.

The concept of DIN 19706 attributes a high value to landscape elements that reduce wind speeds (site and crop-specific soil erosion susceptibility by wind, including windbreaks) [32]. Such landscape elements are forests, hedges, tree rows, windbreaks, etc. It is assumed that the landscape element has a linear effect subject to element height (h) to reduce wind speed and thus protect soils against wind erosion forces. This protective character is likewise effective at the windward side (up to 5 h) as well as at the leeward side (up to 25 h) of the landscape elements [29]. The protection zones are clustered by intervals of five-times height (h), e.g., 0 h –5 h , >5 h –10 h , etc. Typical mean landscape element heights are proposed in DIN 19706 and were lumped together in Schmidt et al. [23] for the SoLoWind model. To overcome the rather general averaging approach of mean landscape element height, we used the digital surface model to extract the heights on a $1 \text{ m} \times 1 \text{ m}$ spatial resolution for each landscape element on a cell base. This approach respects a windbreak differentiation of development stages. Landscape elements such as forests were extracted from the digital elevation model of Lower Austria [52]. In addition to the windbreak data from the Lower Austrian Authority for Land Reform, windbreaks were manually digitalized from orthophotos [47]. We used a weighted approach of windbreak protection zones to include the variations in wind direction and did not only include land-

scape elements perpendicular to the main wind direction according to the mean protection zone (MPZ) module in Schmidt et al. [23].

2.3.2. RWEQ

The WEQ was initially developed by Woodruff and Siddoway [18] and is based on wind tunnel experiments and field measurements. The model was further improved and led to the empirical and process-based RWEQ by Fryrear et al. [19], which was applied in different climate zones for different soil types and scales. It has broad adaptability due to its factorial character [53] because each factor can be modeled individually. The RWEQ models the average soil loss (SL) per period (kg m^{-2}) at a specific point (z) in a field in relation to the non-erodible field border determined by the critical field length (s) in meters (m) at which 63% of the maximum transport capacity is reached:

$$SL = \frac{2z}{s^2} Q_{max} e^{-\left(\frac{z}{s}\right)^2} \quad (1)$$

Q_{max} (kg m^{-1}) is the maximum transport capacity defined by the multiplication of the individual model factors:

$$Q_{max} = 109 * (WF * EF * SCF * K' * COG) \quad (2)$$

where WF is the weather factor (kg m^{-1}), EF is the erodibility factor (dimensionless), SCF is the soil crust factor (dimensionless), K' is the roughness factor (dimensionless), and COG is the combined crop factor (dimensionless). The critical field length is derived by:

$$s = 150.71 * (WF * EF * SCF * K' * COG)^{-0.3711} \quad (3)$$

Weather Factor (WF)

WF is a product of the wind factor W ($\text{m}^3 \text{s}^{-3}$), the ratio of air density (kg m^{-3}) to gravitational acceleration (9.81 m s^{-2}), the dimensionless soil wetness factor (SW), and the dimensionless snow cover factor (SD):

$$WF = W_f * \frac{\rho}{g} * SW * SD \quad (4)$$

W_f is the total sum of daily wind forces within a period:

$$W_f = \frac{\sum_{i=1}^N U_2 (U_2 - U_t)^2}{N} * N_d \quad (5)$$

where U_2 is the wind speed at 2 m height (m s^{-1}), and U_t is the threshold wind speed at 2 m height. We chose the standard threshold of 5 m s^{-1} , which also equals the lower limit of observations in the neighboring country Slovakia [54] that corresponds approximately to the proposed wind speed threshold of Fryrear et al. [10] and that of Skidmore and Woodruff [55] of 5.4 m s^{-1} for the USA. N equals the total number of wind speed observations, and N_d is the total number of days within a period (e.g., monthly).

The air density (ρ) for the measurement location is calculated based on daily measurements of air pressure, temperature, and relative humidity, as follows:

$$\rho = \left(\frac{p_d}{(R_d * T)} \right) + \left(\frac{p_v}{(R_v * T)} \right) \quad (6)$$

where p_d is the pressure of dry air (Pa), R_d is the specific gas constant for dry air ($287.058 \text{ J kg}^{-1} \text{ K}^{-1}$), T is the temperature in (K), p_v is the water vapor pressure (Pa), and R_v is the specific gas constant for water vapor ($461.495 \text{ J kg}^{-1} \text{ K}^{-1}$).

The water vapor pressure (p_v) is the product of the saturation vapor pressure (p_{vs}) and the relative humidity (%), with p_{vs} calculated based on the Tetens equation as:

$$p_{vs} = 6.1078 * 10^{\left(\frac{7.5 * T_c}{T_c + 237.3}\right)} \quad (7)$$

where T_c is the temperature ($^{\circ}\text{C}$); p_d can be calculated as the difference of the absolute air pressure p to p_v :

$$p_d = p - p_v \quad (8)$$

Soil wetness index (SW) is the difference between the soil's water loss by evapotranspiration (ET_p ; mm) and the water gain by rainfall (R ; mm) and irrigation (I ; mm) within the defined period:

$$SW = \frac{ET_p - (R + I) * \frac{R_d}{N_d}}{ET_p} \quad (9)$$

For deriving the potential evapotranspiration, which is relevant for SW , we used the following equation:

$$ET_p = 0.19 * (20 + T_i)^2 * (1 - r_i) \quad (10)$$

where R_d represents the number of rainfall and/or irrigation days within the period, and N_d the number of absolute days within the period. As no information is available regarding irrigation practices within the study region, we set this parameter to 0 mm. T_i is the monthly mean temperature ($^{\circ}\text{C}$), and r_i is the monthly mean relative humidity (%).

SD is the snow cover, where P is the probability of a snow depth greater than 25.4 mm:

$$SD = 1 - P(\text{snow depth} > 25.4 \text{ mm}) \quad (11)$$

As the probability of a snow depth > 25.4 mm increases, SD decreases and thus has a positive effect on reducing WF as snow cover protects topsoil against detachment. If snow depth measurements were not available or erroneous within the meteorological measurements, we substituted the parameter by the assumption 1:10. This means that 1 mm daily mean rainfall at a temperature < 0 $^{\circ}\text{C}$ equals a snow depth of 10 mm [53].

Each of the sub-factors of WF was calculated separately for the meteorological data of the 22 stations using the following equations. Calculated monthly WF s were later interpolated by ordinary kriging with first or second trend removal. Additionally, an annual WF was calculated based on an annual aggregation of each of the sub-factors, as mentioned above and interpolated by ordinary kriging (second trend removal).

Erodibility Factor (EF) and Soil Crust Factor (SCF)

The EF and SCF are derived according to Fryrear et al. [19] by an empirical function based on sand content (Sa ; %), silt content (Si ; %), clay content (Cl ; %), organic matter content (SOM ; %), and calcium carbonate content ($CaCO_3$; %):

$$EF = \frac{29.09 + 0.31 * SA + 0.17 * Si + 0.33 \left(\frac{Sa}{Cl}\right) - 2.59 * SOM - 0.95 * CaCO_3}{100} \quad (12)$$

$$SCF = \frac{1}{1 + 0.0066 * (Cl)^2 + 0.021 * (SOM)^2} \quad (13)$$

Both equations were applied to the features of eBod to result in maps of EF and SCF . As eBod provides the texture classes in the WRB classification scheme, texture classes were transformed to USDA classification using a log-linear transformation. The transformation was realized in R with the package *soiltexture* [56]. We assumed no intra-annual or multi-annual dynamics of EF and SCF . For the EF -RWEQ, we chose a classified color scheme of six classes according to equal intervals of 0.16 from 0 to 1, where 0 to <0.16 is no erodibility and 0.16 to <0.32 is very low et cetera.

Soil Roughness Factor (K')

The soil roughness factor (K'), as a dimensionless factor, considers the soil surface roughness and the soil ridge roughness and is described in detail in Saleh and Fryrear [57]. It includes aggregate/random (RR) and ridge/oriented roughness (K_r). K' can be calculated as:

$$K' = e^{[(R_c * (1.86 * K_r - 2.411 * K_r^{0.934})) - 0.124 * C_{rr}]} \quad (14)$$

RR was converted to chain random roughness (C_{rr}) according to Equation (15).

$$C_{rr} = 17.46 * RR^{0.738} \quad (15)$$

K_r (cm) is dependent on the geometry of ridges as proposed by Zingg and Woodruff [58] in Equation (16) where RH is the ridge height (cm), and RS is the ridge spacing (cm).

$$K_r = 4 * \frac{RH^2}{RS} \quad (16)$$

As in the European RWEQ-map of Borrelli et al. [14], a RR of approx. 2 cm (0.8 inch-es) was set as well as a standard parameter for conventional tillage with plowing and harrowing ($RH = 1.5$ cm, $RS = 14.3$ cm), reduced tillage with gently soil inversion techniques as strip tillage or the reduction of inversion tillage depth ($RH = 2$ cm, $RS = 36$ cm) and no-tillage without soil inversion ($RH = 0.5$ cm, $RS = 36$ cm). Tillage methods are described in detail in Zikeli and Gruber [59].

According to Saleh and Fryrear [57], the soil roughness at any given angle (R_c), related to the orientation of ridges, can be considered as [57]:

$$R_c = 1 - (0.00032 * \theta + 0.000349 * \theta^2 - 0.00000258 * \theta^3) \quad (17)$$

where θ ($^\circ$) is the angle from the direction perpendicular to the ridges.

We used an intermediate θ of 45° .

As no parcel-based agricultural practice information is available, we weighted K' according to the distribution of conventional tillage (47%), reduced tillage (38%), and no-tillage (15%) for Lower Austria [40] to result in a weighted K' for all parcels in the study region. For the modeling approach, we assumed a constant K' all year round.

Combined Crop Factor (COG)

Combined crop factor (COG) was derived from the multispectral Sentinel-2 (S2) data on a monthly scale. The COG factor represents the fraction of vegetation cover scaled from 0 to 1, where 1 corresponds to a completely bare field, and 0 corresponds to a fully covered field with no wind erosion risk. S2 data was clipped to the parcel extent of the corresponding year. Subsequently, the red and near-infrared bands were used to extract the Normalized Differenced Vegetation Index (NDVI) for each S2 scene. All S2 images within recurring months between 2018 and 2020 were averaged to a mean monthly NDVI. The mean monthly NDVI was transformed to the mean monthly fraction of vegetation cover (FVC) by an endmember unmixing approach using the following equation:

$$FVC = \frac{(NDVI - NDVI_{soil})}{(NDVI_{veg} - NDVI_{soil})} \quad (18)$$

The endmembers were $NDVI_{soil}$ and $NDVI_{veg}$, representing the endmember NDVI value for the soil and vegetation spectrum. As we noticed, e.g., asphalt residuals, spoil pile, shelter roofs, and fences within the outlier values, we set $NDVI_{soil}$ and $NDVI_{veg}$ to the 1st and 99.99th percentiles, respectively, to assess only legitimate soil and vegetation endmembers. The effectiveness of vegetation cover to protect soil surfaces was assessed

by an empirical exponential equation by Mezősi et al. [60] (Equation (19)), where wind erosion risk was observed to be close to 0 at an FVC of 60%.

$$COG = e^{-0.077 * FVC} \quad (19)$$

WF and K' were tabularly calculated. Modeling of all factors and Q_{max} and S_L was realized in ESRI ArcGIS Pro 2.7.3 [61].

3. Results and Discussion

3.1. Erodibility and Surface Crust Factor within the Study Region

As erodibility is dependent on soil texture and soil properties, both erodibility maps from DIN 19706 (EF-DIN) and RWEQ (EF-RWEQ) can be compared regarding spatial clusters (Figure 3). The maps show comparable spatial patterns of erodibility, with higher erodibilities in the center of the study region and the upper and lower eastern area. These areas correspond to areas with sandy soil with medium soil organic matter content. However, the class assignment differs, resulting from the different approaches used to assess erodibility. Moreover, classifying EF-RWEQ values into erosion risk groups is subjective. Alternative classifications to the one we used also result in different areas. For example, López et al. [62] classified EF-RWEQ for European soils into the following three classes: $EF < 0.4$ (slightly erodible), $EF 0.4$ to < 0.5 (moderately erodible), and $EF > 0.5$ (highly erodible). That classification rests on Shiyatyi [63], whereat the soil should be represented by a potential erodibility that equals the compensation of erosion. In the present study, 75%, 17%, and 8% of all cells were within these classification classes. A further differentiation by Jugder et al. [64] for Mongolia is based on the country-specific soil classification and natural zones. The classification uses class breaks of $EF \leq 0.28$ (very low), $EF > 0.28$ to ≤ 0.32 (low), $EF > 0.32$ to ≤ 0.35 (medium), $EF > 0.35$ to ≤ 0.40 (high), and $EF > 0.40$ (very high), resulting in EF classes covering, respectively, 31%, 18%, 8%, 19%, and 25% of the area. The distribution of erodibility classes of DIN 19706 (Figure 3a) is 3.6% for class 0 (no erodibility), 69.4% for class 1 (very low erodibility), 17.9% for class 2 (low erodibility), 7.1% for class 3 (medium erodibility), 1.8% for class 4 (high erodibility), and 0.1% for class 5 (very high erodibility). According to the equal interval class breaks of 0.166, the distribution for the erodibility fraction of RWEQ (Figure 3b) is 4.3% (0 to < 0.166), 48.0% (0.166 to < 0.32), 39.5% (0.32 to < 0.48), 8.2% (0.48 to < 0.64). Higher EF values were not calculated. The median value for the study region corresponds to class 1 (very low) for DIN 19706 and 0.33 for RWEQ. For EF-RWEQ, the median is slightly higher than that extracted for the study region from the EF raster map in Borrelli et al. [14], which is 0.27 based on a modeling approach with soil properties and covariates based on the ESDAC JRC Soil Database for the same study region.

EF-RWEQ enables a much higher differentiation of erodibility as it provides graduated index values from 0 to 1. Erodibility of DIN 19706 is only calculated by soil texture classes and does not consider absolute proportions of soil texture fractions. Furthermore, EF-RWEQ includes the inorganic carbon content because calcareous soils often cause a higher soil aggregation and thus a lower erodibility in humid zones [65]. Overall, EF-DIN and EF-RWEQ demonstrate that the erodibility within the study region is relatively low with few areas of high and very high erodibility according to EF-DIN. However, the choice of classification scheme (e.g., according to Jugder et al. [64]) may lead one to interpret results differently.

An indicator for soil crusting is only present for RWEQ (SCF-RWEQ). Although its effect has long been documented [65], soil crusting is not considered in DIN 19706. Loamy soils (sandy loams, silty loams) are most vulnerable to crust formation and thus less sensitive to wind erosion than sandy soils. Mean SCF-RWEQ is 0.31, with similarly high index values in such zones that have already a relatively high erodibility (Figures S1 and S2).

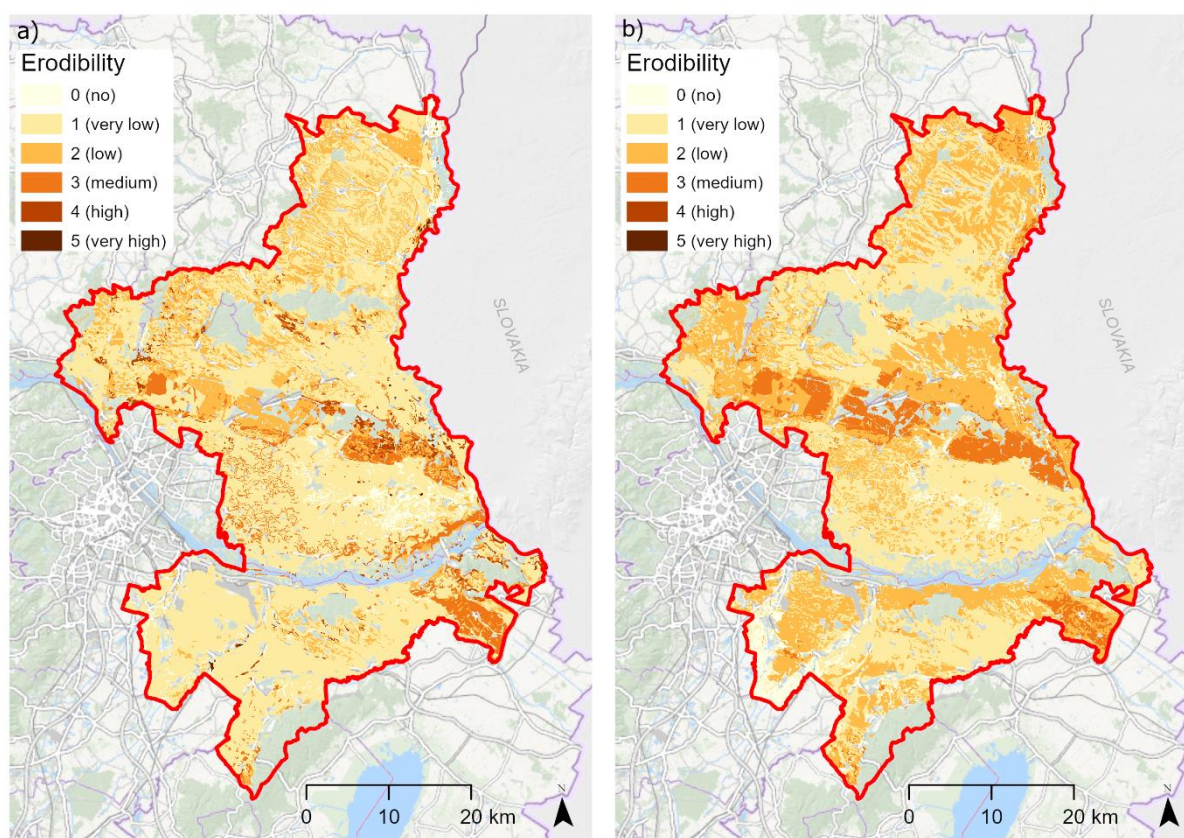


Figure 3. Erodibility maps of DIN 19706 (a) and revised wind erosion equation (RWEQ) (b) based on qualitative classes. Erodibility of RWEQ was classified according to six equal classes (range of 0.16).

3.2. Climate Factors within the Study Region

Mean annual wind speed is the only climate parameter controlling the erosivity of wind in DIN 19706. No additional parameters, such as wind direction, precipitation, evapotranspiration, or soil moisture, are considered in the equation. Thus, it may be expected that wind speed has a high influence on the site-specific soil susceptibility to wind. The climate factor of DIN (CF-DIN) showed little differentiation as most of the values are within the relatively broad classes of >3 to 4 m s^{-1} and >4 to 5 m s^{-1} . However, the absolute mean annual wind speeds were higher in the Danube floodplains and the northern part of the study area (Figure 4a).

Basically, the WF of RWEQ (WF-RWEQ) is rather a weather than a climate factor as it includes more detailed information relating to weather records. Next to the daily wind speeds, a soil wetness factor and a snow depth factor are included. Hence, it considers the drying of soils proportional to the evapotranspiration to precipitation ratio. Regarding the WF-RWEQ, the highest WF can be found in the northern and southern parts of the study region, whereas the center has a relatively lower WF (Figure 4b). The mean annual WF for the study region is 549.5 kg m^{-1} , which is lower than the mean annual potential WF (without topsoil moisture adjustment) modeled for the European Union (643 kg m^{-1}) by Borrelli et al. [14].

The comparison of the mean annual wind speeds used in DIN 19706 and the WF of RWEQ lead to considerable differences based on the different parameters included in the factors. For WF, rainfall and snow depth might compensate high wind speeds in several areas. Vice versa, areas with lower wind speeds remain drier; hence they have higher WF values. As such, the ancillary factors of WF have a moderating effect and, thus, level the value ranges. Contradictory for the mean annual wind speeds in DIN 19706, the lowest and highest values differ with a factor of 2, which is much higher than for WF.

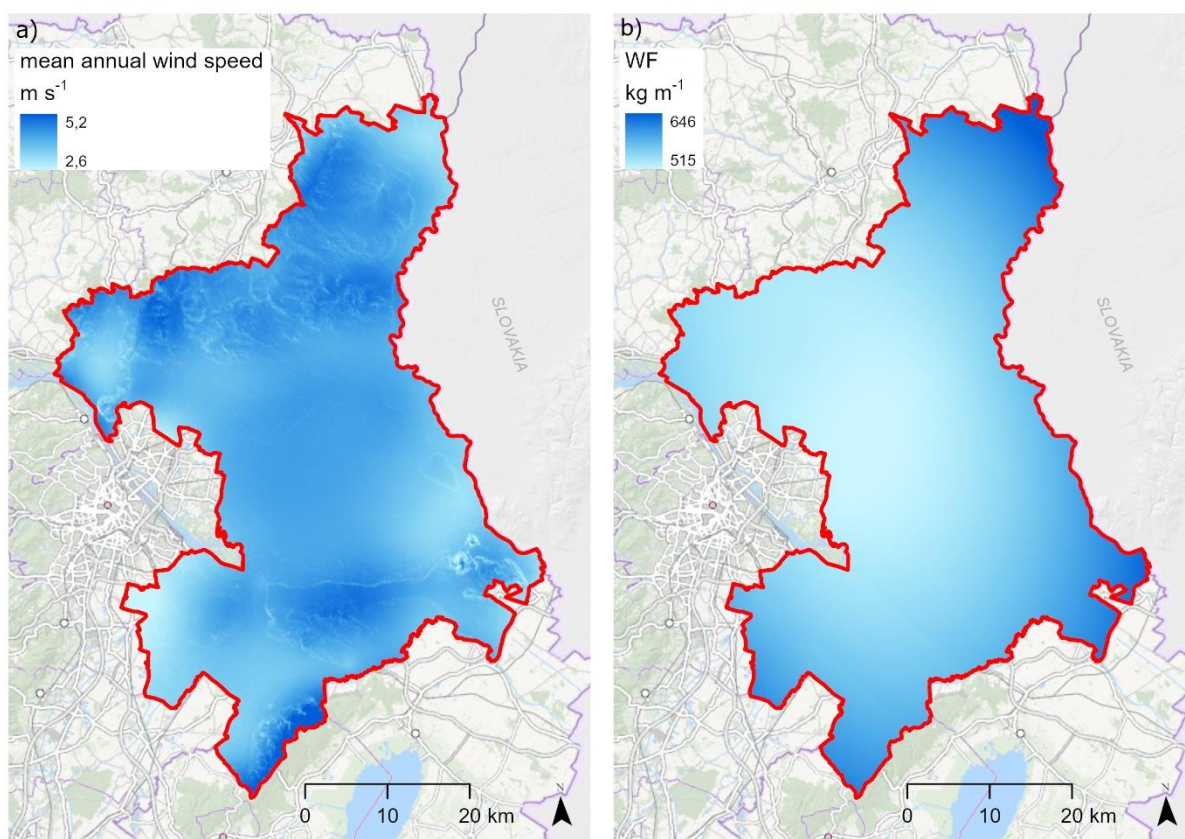


Figure 4. Climate/weather factor of (a) DIN 19706, represented by mean annual wind speed (m s^{-1}), and (b) weather factor (WF) of revised wind erosion equation (kg m^{-1}) by Equation (4).

3.3. Comparison of the Wind Erosion Risk Maps

The study region has a mean annual SL-RWEQ rate of $3.7 \text{ t ha}^{-1} \text{ yr}^{-1}$. The medium class of DIN 19706 of the study region is 0 (no wind erosion risk). It is assumed that the category “no wind erosion risk” coincides with a soil loss rate of $<2 \text{ t ha}^{-1}$. This rate is generally considered the soil formation rate, with a weathering rate of 10 cm within one century [66]. Overall, the erosion risk in the study region is relatively low according to the two modeling approaches, yet the relatively high erosion risk by wind is locally noticeable. Areas prone to wind erosion can be found in the three marked (black outlined rectangle) parts of the study region in Figure 5 for the wind erosion risk assessment of DIN 19706 and the soil loss estimation by RWEQ (SL-RWEQ).

As spatial trends and similarities are recognizable for the wind erosion risk and soil loss maps of both approaches (Figure 5) but not for the climate and weather factor (Figure 4), it is assumed that the influence of erodibility is stronger than that of climate. The comparison of the risk assessments based on DIN 19706 and RWEQ demonstrates a different grade of detail (Figure 5), which is caused by the different approaches and the use of different spatial resolutions of input data. Furthermore, DIN 19706 models wind erosion risk on a single annual scale (e.g., 2020), while RWEQ uses long-term data to model the average multi-annual soil loss.

The three risk zones in Figure 5 correspond well with a former wind erosion risk assessment of 1972 [16], mainly based on the topsoil characteristic of soils and intense wind velocities. Furthermore, the spatial patterns of both maps (Figure 5) are in accordance with the soil vulnerability to wind erosion in the adjacent region (Bratislava) of Slovakia to the east [54]. Hence, the spatial patterns of soil erosion risk are relatively comparable, irrespective of the choice of wind erosion risk assessment or model. As DIN 19706 and RWEQ assess soil erosion risk with a different approach (qualitative vs. quantitative), the distribu-

tion of classes is not directly comparable (Figure 6). However, Figure 6 demonstrates that the majority (>90%) of the cells are within the first three classes in both approaches.

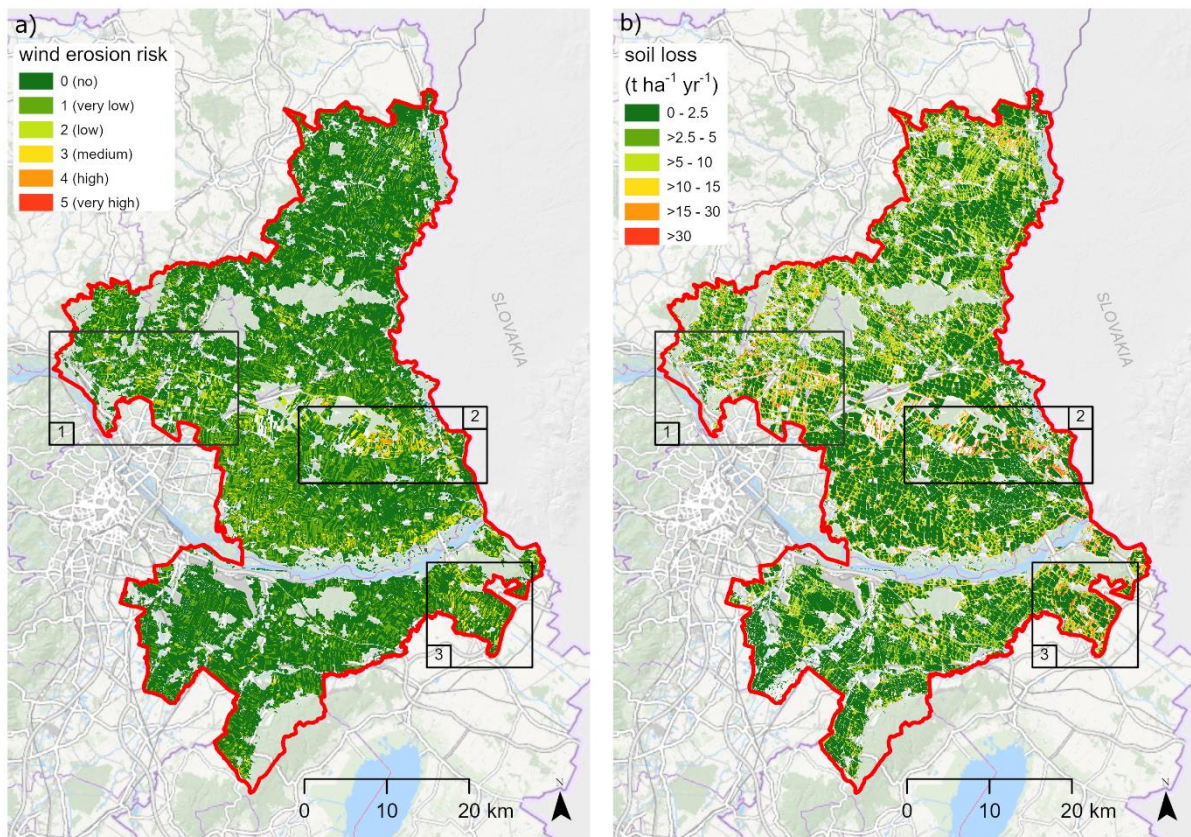


Figure 5. (a) Wind erosion risk for the year 2020 based on DIN 19706 and (b) average multi-annual soil loss in $t\ ha^{-1}\ yr^{-1}$ modeled with revised wind erosion equation.

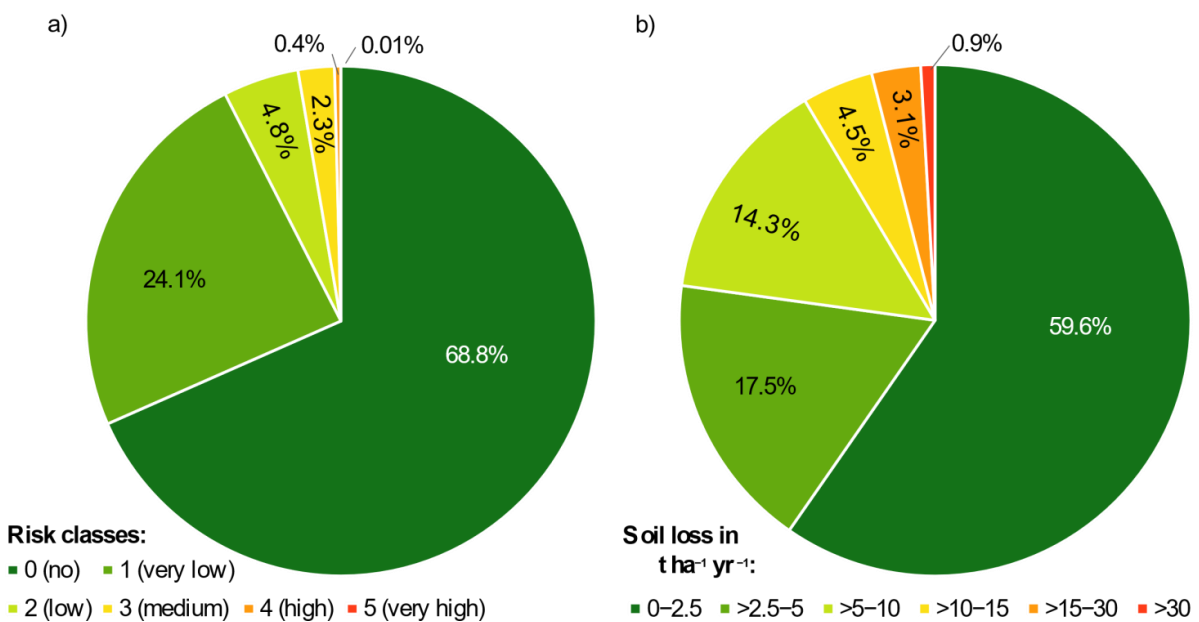


Figure 6. Distribution of (a) risk classes assessed by DIN 19706 and (b) wind erosion soil loss in $t\ ha^{-1}\ yr^{-1}$ per soil loss class modeled with the revised wind erosion equation (RWEQ).

Aggregating cell values into average field soil loss rates resulted in more apparent patterns for the RWEQ soil loss map (Figure S3). The distribution of the proportion of wind erosion risk or soil loss class on a field basis is presented in Table 2. It is evident that 80.4% of all fields in the study region are classified as of no risk according to DIN 19706, while the RWEQ modeling results show that soil loss rates less than or equal to $2.5 \text{ t ha}^{-1} \text{ yr}^{-1}$ were modeled for more than 50% of the fields.

As shown in Table 2, a wind erosion risk of 0 (no) in DIN 19706 does not mean that no wind erosion exists, but soil loss rates might be so low that they are not detrimental to the environment. Nevertheless, according to RWEQ, approx. 23% of all fields have soil loss rates $> 5 \text{ t ha}^{-1} \text{ yr}^{-1}$, which are not neglectable because soil formation rates are estimated to be between 1 and $4.5 \text{ t ha}^{-1} \text{ yr}^{-1}$ [67] and thus lower than soil losses. Instead of considering the soil formation rates, the classification after Zachar [68] (see Table 2) is based on the thickness of the topsoil layer and thus related to the estimated loss of nutrients over time from the topsoil.

Table 2. Distribution of the proportion of wind erosion risk according to DIN 19706 (WER-DIN) and soil loss classes according to revised wind erosion equation (SL-RWEQ) on a field base.

WER-DIN	% of Fields	SL-RWEQ $\text{t ha}^{-1} \text{ yr}^{-1}$	% of Fields	SL-RWEQ in $\text{t ha}^{-1} \text{ yr}^{-1}$ Classified after Zachar [68]	% of Fields
0 (no)	80.4	0–2.5	53.7	0–0.5 (weak)	17.1
1 (very low)	15.3	>2.5–5	22.9	>0.5–5 (slight)	59.5
2 (low)	3.1	>5–10	16.1	>5–15 (moderate)	20.3
3 (moderate)	1.1	>10–15	4.2	>15–50 (severe)	2.9
4 (high)	0.2	>15–30	2.5	>50–200 (very severe)	0.1
5 (very high)	0.0	>30	0.6	>200 (catastrophic)	0

The modeled mean soil annual soil loss by wind (SL-RWEQ) is almost 2.5-times higher than the modeled soil loss by water ($1.5 \text{ t ha}^{-1} \text{ yr}^{-1}$) for the same region (Niederösterreichisches Flach- und Hügelland, Lower Austrian low and hilly country) [69]. As shown by these numbers, wind erosion is more problematic in the eastern part of Austria than water erosion due to the natural characteristics (flat area, light soils, high agricultural productivity). Erosion by water dominates in other Austrian regions (e.g., pre-alpine forelands) as indicated in various modeling approaches [67,70].

3.4. Individual Consideration of Wind Erosion Parameters

Contrary to DIN, RWEQ can model soil loss on a monthly scale by including the WF and the COG factor for each month. All other factors are assumed to be relatively constant within a year. The intra-annual distribution of WF-RWEQ showed an increasing trend of WF from winter to summer, with a maximum WF value of 61.0 kg m^{-1} in July (Figure S4). The average monthly WF is 46.5 kg m^{-1} . Monthly WF-RWEQ values are listed in Table 3. May has the highest mean WF-RWEQ, which can be explained by the highest wind forces within a year. Generally, the northern part of the study region and the border area to Slovakia have the highest WF values each month. Likewise, these parts of the region have the lowest observed mean rainfall records in the study area. Related to rainfall, snow depths are lowest in the north of the study region. Indeed, wind speeds are relatively high in winter and spring, though concurrent high snow depths from November to March scale down that factor during these seasons. This seasonality contrasts with the generally highest WF in January and March in Europe [14].

The mean monthly COG factor for the study region is 0.19, with the highest value of 0.24 in August. This can be explained by crop harvesting activities at the end of July/beginning of August, resulting in a high combined crop cover. The monthly distribution of COG factors is displayed in Figure S5.

The use of monthly parameters resulted in monthly soil loss maps by RWEQ (Figure 7), with a monthly mean of $0.3 \text{ t ha}^{-1} \text{ month}^{-1}$. Corresponding statistical parameters are

shown in Table 4. The risk zones marked in Figure 5 are continuously visible throughout the year. However, the estimated monthly soil loss rates vary by month, with a peak in soil loss in August.

Table 3. Modelled monthly descriptive statistics (minimum, maximum, mean) of the weather factor (WF) of the revised wind erosion equation for the study region.

Month	Min WF	Max WF	Mean WF
	kg m ⁻¹		
January	28.1	52.6	39.5
February	36.2	41.9	38.2
March	45.4	52.2	48.1
April	47.2	53.5	49.7
May	49.7	55.9	51.7
June	47.2	55.1	49.8
July	45.5	61.0	49.3
August	45.5	58.1	48.9
September	42.3	54.4	45.9
October	44.6	54.7	48.5
November	41.7	55.2	44.7
December	41.6	48.9	43.7

Table 4. Statistical parameters of the modeled monthly soil loss in t ha⁻¹ month⁻¹ by the revised wind erosion equation.

Month	Modeled Soil Loss in t ha ⁻¹ month ⁻¹				
	Mean	Standard Deviation	Median	90th Percentile	99th Percentile
January	0.35	0.64	0.14	0.88	2.88
February	0.27	0.4	0.14	0.62	1.89
March	0.40	0.66	0.17	1.00	3.10
April	0.35	0.67	0.09	0.95	3.15
May	0.26	0.56	0.04	0.74	2.57
June	0.18	0.4	0.05	0.46	1.88
July	0.39	0.82	0.12	0.97	3.88
August	0.49	0.93	0.17	1.26	4.39
September	0.42	0.74	0.17	1.04	3.36
October	0.39	0.65	0.18	0.97	2.99
November	0.27	0.44	0.12	0.67	2.1
December	0.24	0.4	0.11	0.58	1.85

Obviously, vegetation cover has a high impact on soil protection as the seasonal line of soil loss is opposed to the fraction of vegetation cover (Figure 8). This fact was also observed by Frielinghaus et al. [71] and Jiang et al. [72], who used very similar relationships to the one by Mezósi et al. [60] that we used in this study. This interdependency means that situations with relatively sparsely covered soils and simultaneously high WFs (such as in August) cause high soil losses. High WFs cannot effectively erode soil when fields are covered by vegetation (e.g., May/June; Figure S6). Please note that the indexes and values in Figure 8 are normalized based on the maximum and minimum value range by the following equation:

$$\text{Normalization} = \frac{\text{value} - \text{min}}{\text{max} - \text{min}} \quad (20)$$

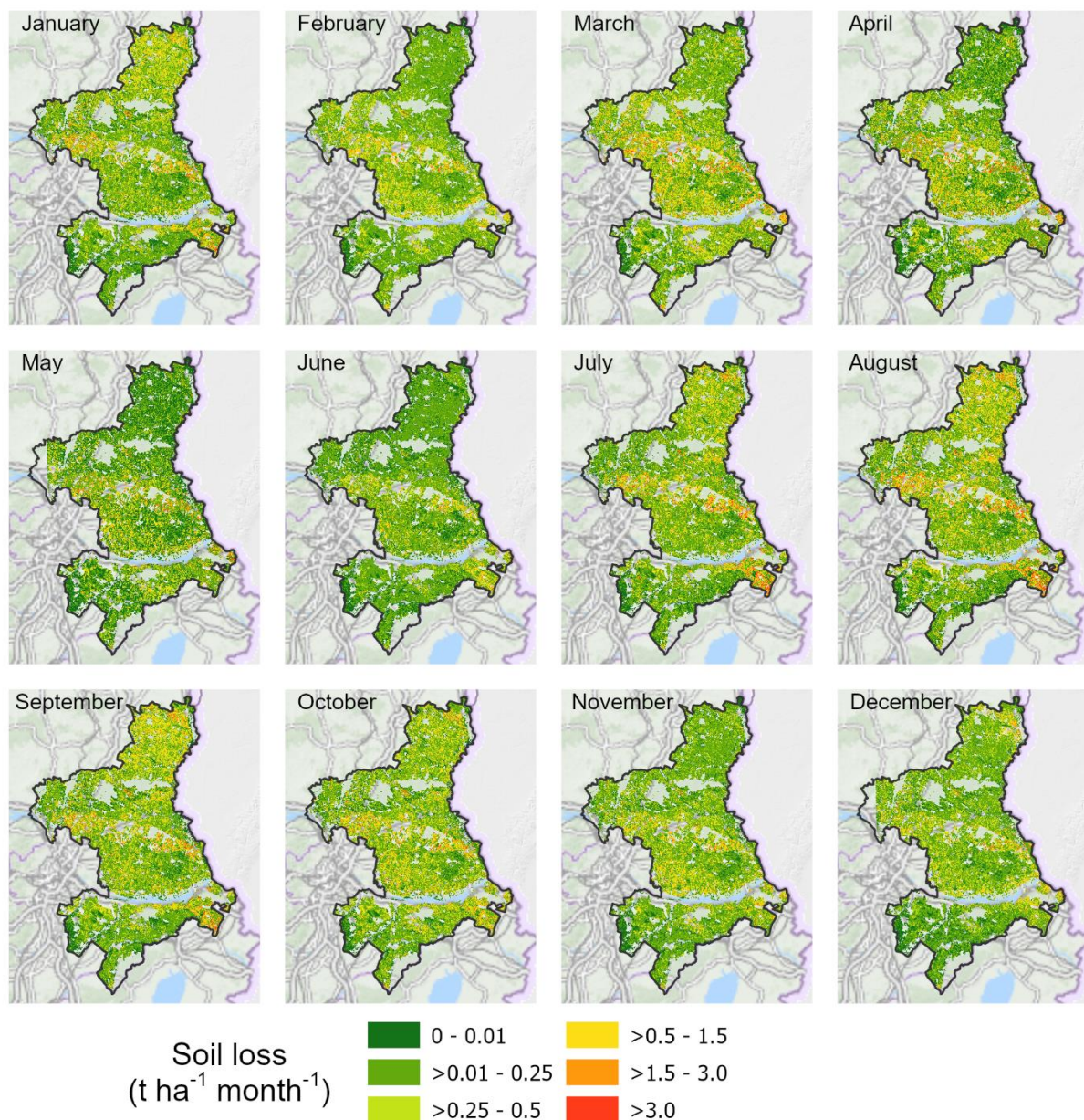


Figure 7. Monthly soil loss (t ha⁻¹ month⁻¹) modeled by revised wind erosion equation for the study region in eastern Austria.

For DIN 19706, a windbreak parameter is considered. This parameter reflects the influence of windbreaks on the windspeed and the reduction of wind erosion in the direct surroundings of any landscape element serving as a windbreak. Windbreaks, at least when not having gaps in their lower part [73], are most effective at the borders of fields, where they are usually installed. The presence of landscape elements towards the center of fields decreases and thus their protective effect is reduced in the center. The inclusion of existing windbreaks within the study region reduced the wind erosion risk for all susceptible fields (Figure 9). As such, windbreaks demonstrate high effectiveness as an erosion measure. In addition, windbreaks have many other benefits for the environment, for example, positive effects on biodiversity, pollination, or nutrient build-up [74]. However, such inclusion introduces additional uncertainty as the protective effect depends on the windbreak's characteristics (e.g., density, porosity, composition). Furthermore, the analysis implies that the effect of including such parameters might be leveled by higher wind erosion risk (see Figure 9).

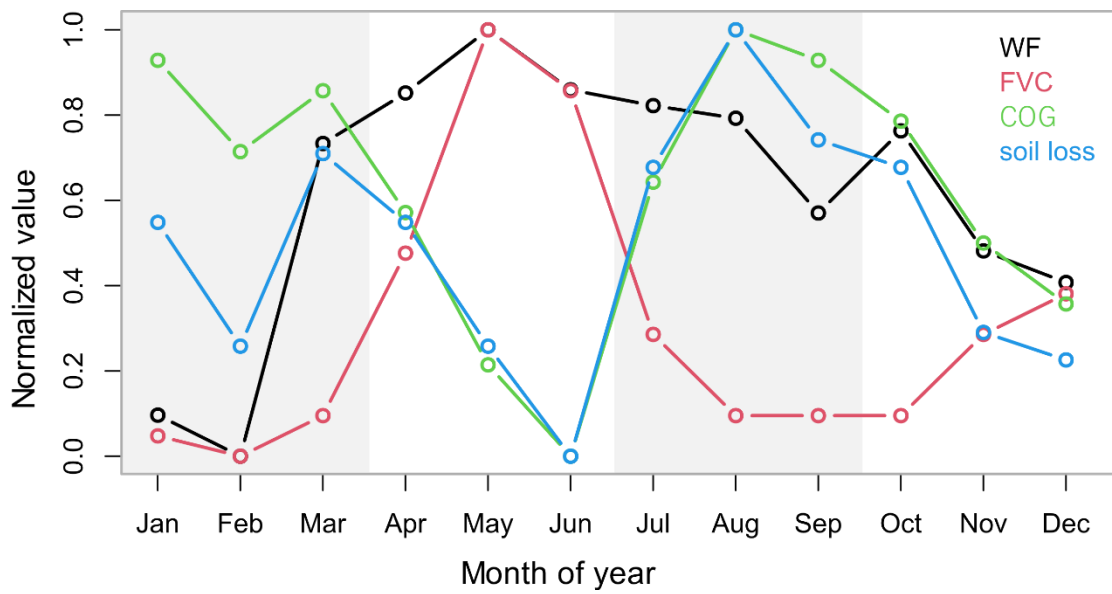


Figure 8. Monthly variation of revised wind equation factors and soil loss on a max-min-normalized scale (see Equation (20)). Abbreviations: WF, weather factor; FVC, mean monthly fraction of vegetation cover; COG, combined crop factor.

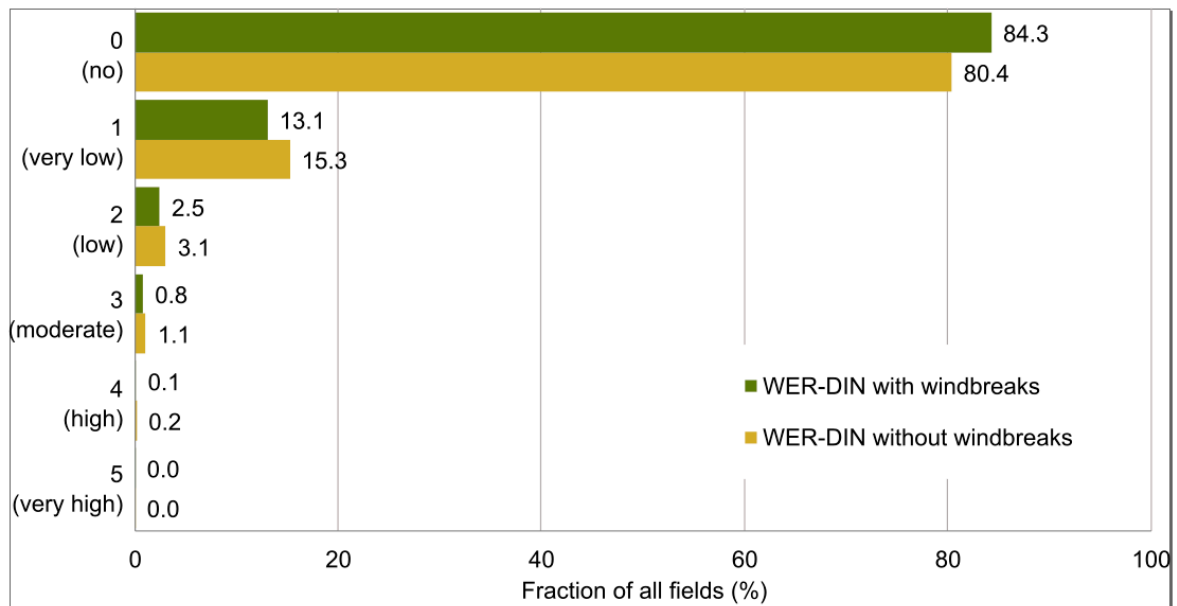


Figure 9. Alteration of the percentage of wind erosion risk of fields within the study by including windbreaks in the risk assessment approach.

3.5. Classification and Severity Classes of Erosion Rates in Quantitative Modeling

The annual soil erosion map modeled by RWEQ was classified according to selected classification schemes [68,75–77]. Results show that, irrespective of the chosen classification scheme, all maps were able to identify the spatial risk zones (Figure 10) already discussed in Section 3.3 (Figure 5), though with a different degree of severity. The relative distribution of raster cells is listed in Table S4.

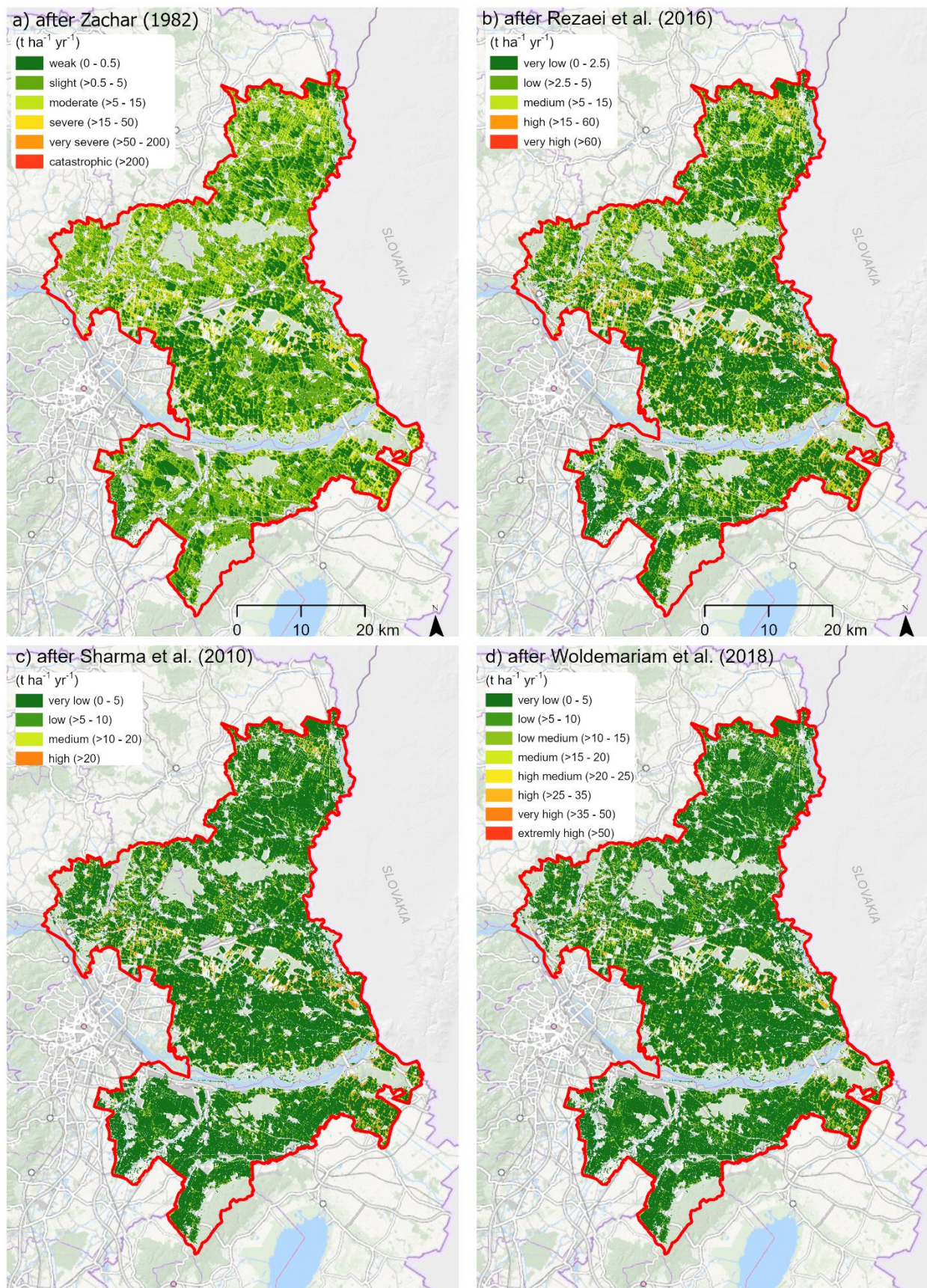


Figure 10. Different perceptions of soil erosion risk according to the choice of the classification scheme and severity classes. Classification schemes do not explicitly use wind erosion but general erosion classification limits (except [75]).

The modeled mean annual soil loss rate by RWEQ of $3.7 \text{ t ha}^{-1} \text{ yr}^{-1}$ can thus be categorized as “slight”, according to Zachar [68]. According to Sharma [76], Rezaei et al. [75], and Woldemariam et al. [77], it is considered as “low”. As such, all classification schemes can categorize the wind erosion risk by a similar qualitative severity class.

The choice of the proper classification scheme for soil loss rates is highly expert knowledge-based and subjective, as is the classification scheme for erodibility and weather factor maps. As discussed in Section 3.1, the setting of erodibility classes is dependent on different rationales, such as the balance of erodibility and compensation of erosion, or controlled by country-specific environmental characteristics. This circumstance should increase the caution in interpreting soil erodibility or soil risk maps.

The interpretability of soil loss rates is often controlled by the choice of the soil erosion classification scheme and assignment of severity classes. The literature does not deal with a common standard of classification that can be misleading in categorizing a study area as prone or non-prone to wind erosion. Furthermore, erosion maps may be manipulated for a selected target audience (e.g., choosing an optimistic or pessimistic classification scheme). The number of classes is inconsistent among different classification methods. More classes may lead to a higher differentiation, whereas a low number of classes (e.g., three to four classes) can easily serve as either optimistic or pessimistic. At least most of the classification schemes have similar ranges of soil loss rates in the class moderate/medium erosion risk.

Thus, a demand for defining a common setting for erosion classification is needed to avoid a misinterpretation of the results and make the results of different study areas and/or countries comparable. Comparing soil loss rates between different regions must be carried out carefully as soil erosion by wind may affect soils differently, and therefore high erosion rates at one spot may be classified differently on another spot. A reasonable reference for the formulation or the choice of an appropriate classification system might be the soil formation rate, which varies regionally. Nevertheless, none of the mentioned systems refers to such a formation rate. Soil formation rates vary considerably with climate and parent material; there is no explicit calculation known for the study region. For Europe, Verheijen et al. [78] reviewed the literature on soil formation rates and found values between $0.3 \text{ t ha}^{-1} \text{ yr}^{-1}$ and $1.4 \text{ t ha}^{-1} \text{ yr}^{-1}$. Sustainable soil management should be aimed at reducing soil erosion rates below the respective soil formation rates. In this concern, the classification schemes for wind erosion rates as discussed herein should be refined as the values for soil formation rates correspond to classes denoted as slight or no wind erosion risk.

3.6. Limitations of DIN19706 and RWEQ

DIN 19706 is missing some crucial factors, as already discussed in Schmidt et al. [23], which has led to a modified model called SoLoWind. SoLoWind includes the variations of wind direction and a parameter regarding field length and proposes a way to substitute the site-specific land use information by satellite data (COV-factor) if such information is not available. Neither the climate factor nor the EF of DIN 19706 consider soil moisture characteristics. Merely using a certain wind speed threshold and a preceding non-precipitation phase (e.g., 48 h) only partially includes moisture patterns. In SoLoWind, the EF is modified by including site-specific soil moisture indices of topsoil based on Ellenberg’s indicator values [79]. These values are an ecology index that includes seven gradients, one of which is the nine classes of F-value for soil humidity or moisture. However, SoLoWind has only been applied once in Saxony, Germany, and thus is not as widely applied as DIN19706. Unlike DIN 19706, RWEQ includes a soil moisture index in the form of the soil wetness factor. DIN 19706 only considers long-term wind speeds but neglects erosive winds. Therefore, extreme events with high wind speeds are not considered at all. Initially, both approaches do not consider variations in wind direction. Even though, in our study region, erosive winds have a noticeable tendency to be in a northwestern direction (35%), other directions should not be neglected (e.g., southeasterly winds: 27%). These multidirectional winds affect not only the windbreaks but also influence the orientation of fields. However, the

orientation of fields is partly assessed in the K' -factor of RWEQ, as the orientation of ridges may be considered. A parcel-based approach for an extensive study region such as the Pannonian Basin is hampered due to missing information relating to topsoil cultivation. Other qualitative risk assessments are often linked to specific study areas and/or local datasets. Models such as WEELS [80] or WEPS have a high data demand or are only applicable to single events.

In a future step, we envisage the derivation of a roughness parameter from a spatially high-resolution digital surface model. Additionally, we are currently conducting in-field roughness measurements to improve the understanding of roughness parameters. Furthermore, wind erosion measurements at different distances to windbreaks and the botanical description of windbreaks (e.g., density, composition) are currently being conducted at study plots in eastern Austria to better understand, integrate, and quantify the effectiveness of windbreaks. The aim is to aggregate the measured and mapped information into the percent of upwind velocity (PUV) factor, thus describing the barrier effect of planted windbreaks to the RWEQ [19].

4. Conclusions

Qualitative risk assessments are often used because they require less complex and comprehensive data than empirical, process-based, or physical wind erosion models. Comparing the qualitative DIN 19706 approach and the empirical and process-based RWEQ model resulted in comparable spatial patterns of soil erodibility. However, the climatic parameters of both models are not comparable as they are based on entirely different relationships and input parameters. Both models identified main risk zones within the study region in the Pannonian Basin of eastern Austria, at similar locations, irrespective of the classification scheme used. Furthermore, based on RWEQ, seasonal trends were noticeable, with the highest wind erosion risk in August. Because vegetation cover reduces soil erosion efficiently, the planting of cover crops, which needs to be established during seasons with high weather factors and commonly bare soils, is a proven practice against soil loss by wind.

The two models follow different modeling strategies (e.g., annual vs. monthly approach, focus on land use vs. climate). Regarding the comparability of spatial patterns, DIN 19706 can be seen as a valuable tool for gaining a first impression about the susceptibility of soils due to wind erosion, although the absolute class assignment is debatable. RWEQ can serve to delineate risk zones and provides a quantification of soil loss that might be helpful for their categorization. However, an improved and more realistic wind erosion estimation may be enabled by either a modification of RWEQ by a windbreak parameter or an in-depth quantification of DIN 19706 risk. Moreover, other qualitative risk assessment and quantitative models should also be considered alongside DIN 19706 and RWEQ to evaluate their comparability.

Supplementary Materials: The following are available online at <https://www.mdpi.com/article/10.3390/land10090974/s1>, Table S1: List of meteorological stations, Table S2: Soil erodibility matrix, Table S3: Assignment of protection classes of different types of fruits, Figure S1: Flow chart of DIN 19706, Figure S2: Soil crust factor (SCF) map of RWEQ, Figure S3: Mean soil loss per field based on RWEQ, Figure S4: Interpolated weather factor (WF) of RWEQ, Figure S5: Monthly COG factor of RWEQ, Figure S6: Monthly fraction of vegetation cover derived by Sentinel-2 data, Table S4: Distribution of soil erosion classes according to different classification schemes

Author Contributions: Conceptualization, S.S., K.M., T.W., L.L., B.K., W.C. and P.S.; methodology, S.S.; formal analysis, S.S.; investigation, S.S.; writing—original draft preparation, S.S.; writing—review and editing, S.S., K.M., T.W., L.L., B.K., W.C. and P.S.; visualization, S.S. and T.W.; supervision, K.M.; project administration, K.M.; funding acquisition, K.M.; All authors have read and agreed to the published version of the manuscript.

Funding: This research was funded by the Austrian Climate and Energy fund within Austrian Climate Research Programme (ACRP) 11, grant number N° KR18AC0K14642, as part of the research project EROWIN (project number B960199).

Data Availability Statement: The data presented in this study are available on request from K. Michel. The data are not publicly available due to data privacy policy.

Acknowledgments: This work was supported by the Austrian Climate and Energy fund within Austrian Climate Research Programme (ACRP) 11 (grant number N° KR18AC0K14642). The authors would like to thank all data providers for making their data available for that research. We appreciate the support of C. Aufreiter for extracting the windbreak heights and M. Biberacher for providing the mean annual wind speeds. We would also like to thank the three anonymous referees.

Conflicts of Interest: The authors declare no conflict of interest.

References

- Arshad, M.A.; Martin, S. Identifying critical limits for soil quality indicators in agro-ecosystems. *Agric. Ecosyst. Environ.* **2002**, *88*, 153–160. [[CrossRef](#)]
- Pimentel, D.; Burgess, M. Soil Erosion Threatens Food Production. *Agriculture* **2013**, *3*, 443–463. [[CrossRef](#)]
- Jie, C.; Jing-zhang, C.; Man-zhi, T.; Zi-tong, G. Soil degradation: A global problem endangering sustainable development. *J. Geogr. Sci.* **2002**, *12*, 243–252. [[CrossRef](#)]
- Commission of the European Communities. *Proposal for a Directive of the European Parliament and of the Council Establishing a Framework for the Protection of Soil and Amending Directive 2004/35/EC: /* COM/2006/0232 Final—COD 2006/0086 */*; Commission of the European Communities: Brussels, Belgium, 2006.
- Prävălie, R.; Patriche, C.; Borrelli, P.; Panagos, P.; Roşca, B.; Dumitraşcu, M.; Nita, I.-A.; Săvulescu, I.; Birsan, M.-V.; Bandoc, G. Arable lands under the pressure of multiple land degradation processes. A global perspective. *Environ. Res.* **2021**, *194*, 110697. [[CrossRef](#)]
- Ravi, S.; D’Odorico, P.; Breshears, D.D.; Field, J.P.; Goudie, A.S.; Huxman, T.E.; Li, J.; Okin, G.S.; Swap, R.J.; Thomas, A.D.; et al. Aeolian Processes and the Biosphere. *Rev. Geophys.* **2011**, *49*. [[CrossRef](#)]
- Funk, R.; Reuter, H.I. Wind Erosion. In *Soil Erosion in Europe*; Boardman, J., Poesen, J., Eds.; Wiley: Chichester, UK; Hoboken, NJ, USA, 2006; pp. 563–582. ISBN 0470859105.
- Borrelli, P.; Alewell, C.; Alvarez, P.; Anache, J.A.A.; Baartman, J.; Ballabio, C.; Bezak, N.; Biddoccu, M.; Cerdà, A.; Chalise, D.; et al. Soil erosion modelling: A global review and statistical analysis. *Sci. Total Environ.* **2021**, *780*, 146494. [[CrossRef](#)]
- Chepil, W.S.; Woodruff, N.P. The Physics of Wind Erosion and its Control. *Adv. Agron.* **1963**, *15*, 211–302. [[CrossRef](#)]
- Fryrear, D.W.; Bilbro, J.D.; Saleh, A.; Schomberg, H.; Stout, J.E.; Zobeck, T.M. RWEQ: Improved wind erosion technology. *J. Soil Water Conserv.* **2000**, *55*, 183–189.
- Shao, Y. *Physics and Modelling of Wind Erosion*; Springer: Dordrecht, The Netherlands, 2009; ISBN 9781402088940.
- Borrelli, P.; Ballabio, C.; Panagos, P.; Montanarella, L. Wind erosion susceptibility of European soils. *Geoderma* **2014**, *232–234*, 471–478. [[CrossRef](#)]
- Borrelli, P.; Panagos, P.; Ballabio, C.; Lugato, E.; Weynants, M.; Montanarella, L. Towards a Pan-European Assessment of Land Susceptibility to Wind Erosion. *Land Degrad. Develop.* **2016**, *27*, 1093–1105. [[CrossRef](#)]
- Borrelli, P.; Lugato, E.; Montanarella, L.; Panagos, P. A New Assessment of Soil Loss Due to Wind Erosion in European Agricultural Soils Using a Quantitative Spatially Distributed Modelling Approach. *Land Degrad. Develop.* **2017**, *28*, 335–344. [[CrossRef](#)]
- Wendelberger, G. *Die Restwälder der Parndorfer Platte im Nordburgenland: Die Natürlichen Voraussetzungen Standortgemässer Wiederaufforstungen*; Amt d. Burgenländ. Landesregierung, Landesarchiv—Landesbibliothek: Eisenstadt, Austria, 1955.
- Strauss, P.; Klaghofer, E. Austria. In *Soil Erosion in Europe*; Boardman, J., Poesen, J., Eds.; Wiley: Chichester, UK; Hoboken, NJ, USA, 2006; pp. 205–212. ISBN 0470859105.
- Klik, A. Wind Erosion Assessment in Austria Using Wind Erosion Equation and GIS. Unpublished. 2003.
- Woodruff, N.P.; Siddoway, F.H. A Wind Erosion Equation. *Soil Sci. Soc. Am. J.* **1965**, *29*, 602. [[CrossRef](#)]
- Fryrear, D.; Saleh, A.; Bilbro, J.D.; Schomberg, H.; Stout, J.E.; Zobeck, T.M. Revised wind erosion equation (RWEQ). Wind Erosion and Water Conservation Research Unit, USDA-ARS, Southern Plains Area Cropping Systems Research Laboratory. *Tech. Bull.* **1998**, *1*, 36–51.
- Tatarko, J.; Wagner, L.; Fox, F. The Wind Erosion Prediction System and its Use in Conservation Planning. In *Bridging among Disciplines by Synthesizing Soil and Plant Processes*; Wendroth, O., Lascano, R.J., Ma, L., Eds.; American Society of Agronomy and Soil Science Society of America: Madison, WI, USA, 2019; pp. 71–101. ISBN 9780891183655.
- Hagen, L.J. A wind erosion prediction system to meet user needs. *J. Soil Water Conserv.* **1991**, *46*, 106–111.
- Jarrah, M.; Mayel, S.; Tatarko, J.; Funk, R.; Kuka, K. A review of wind erosion models: Data requirements, processes, and validity. *Catena* **2020**, *187*, 104388. [[CrossRef](#)]
- Schmidt, S.; Meusburger, K.; Figueiredo, T.; Alewell, C. Modelling Hot Spots of Soil Loss by Wind Erosion (SoLoWind) in Western Saxony, Germany. *Land Degrad. Develop.* **2017**, *28*, 1100–1112. [[CrossRef](#)]

24. Le Bissonnais, Y.; Montier, C.; Jamagne, M.; Daroussin, J.; King, D. Mapping erosion risk for cultivated soil in France. *Catena* **2002**, *46*, 207–220. [[CrossRef](#)]
25. van Gool, D.; Tille, P.J.; Moore, G.A. *Land Evaluation Standard Aluation Standards for Land r ds for Land Resource Mapping: Assessing ce Mapping: Assessing Land Qualities and Determining Land Capability in South-Western Australia*; Department of Primary Industries and Regional Development: Perth, Australia, 2005.
26. Department of Agriculture and food. *Report Card on Sustainable Natural Resource Use in Agriculture: Status and Trend in the Agricultural Areas of the South-West of Western Australia*; Department of Primary Industries and Regional Development: Perth, Australia, 2013.
27. Středová, H.; Podhrázká, J.; Chuchma, F.; Středa, T.; Kučera, J.; Fukalová, P.; Blecha, M. The Road Map to Classify the Potential Risk of Wind Erosion. *ISPRS Int. J. Geo-Inf.* **2021**, *10*, 269. [[CrossRef](#)]
28. Négyesi, G.; Lóki, J.; Buró, B.; Bertalan-Balázs, B.; Pásztor, L. Wind erosion researches in Hungary—past, present and future possibilities. *HunGeoBull* **2019**, 223–240. [[CrossRef](#)]
29. DIN German Institute for Standardisation. *DIN 19706:2013-02, Bodenbeschaffenheit_—Ermittlung der Erosionsgefährdung von Böden Durch Wind*; Beuth Verlag GmbH: Berlin, Germany, 2013.
30. Deumlich, D.; Funk, R.; Kiesel, J.; Reuter, H.I.; Thiere, J.; Völker, L. Anwendung der “vergleichsmethode standort (vermost)” zur bewertung der erosionsgefährdungspotenziale als datenbasis für förderinstrumente am beispiel des landes Brandenburg: Application of the site comparison method (vermost) to assess the potential erosion risk as a basis to examine instruments of environmental policy—The example of Brandenburg. *Arch. Agron. Soil Sci.* **2004**, *50*, 259–271. [[CrossRef](#)]
31. Funk, R.; Deumlich, D.; Steidl, J. GIS Application to Estimate the Wind Erosion Risk in the Federal State of Brandenburg. In *Soil Erosion Research for the 21st Century*; American Society of Agricultural and Biological Engineers: Honolulu, HI, USA, 2001. [[CrossRef](#)]
32. Funk, R.; Deumlich, D.; Völker, L.; Steidl, J. GIS application to estimate the wind erosion risk in the Federal State of Brandenburg. In *Wind Erosion and Dust Dynamics: Observations, Simulations, Modelling*; Goossens, D., Riksen, M., Eds.; Wageningen University and Research Centre, Department of Environmental Sciences, Erosion and Soil and Water Conservation Group: Wageningen, The Netherlands, 2004; pp. 139–149. ISBN 90-6754-813-8.
33. Steininger, M.; Wurbs, D. *Bundesweite Gefährdung der Böden durch Winderosion und Bewertung der Veränderung infolge des Wandels klimatischer Steuergrößen als Grundlage zur Weiterentwicklung der Vorsorge und Gefahrenabwehr im Bodenschutzrecht*; Umweltbundesamt: Dessau-Roßlau, Germany, 2017.
34. Funk, R. Assessment and Measurement of Wind Erosion. In *Novel Methods for Monitoring and Managing Land and Water Resources in Siberia*; Mueller, L., Sheudshen, A.K., Eulenstein, F., Eds.; Springer International Publishing: Cham, Switzerland, 2016; pp. 425–449. ISBN 978-3-319-24407-5.
35. Geoland. Digitales Geländemodell (DGM) Österreich 10 m × 10 m. Available online: <https://www.data.gv.at/katalog/dataset/land-ktm-digitales-gelandemodell-dgm-osterreich> (accessed on 17 May 2021).
36. Hiebl, J.; Reisenhofer, S.; Auer, I.; Böhm, R.; Schöner, W. Multi-methodical realisation of Austrian climate maps for 1971–2000. *Adv. Sci. Res.* **2011**, *6*, 19–26. [[CrossRef](#)]
37. ZAMG. Klimamittel 1981–2010. Available online: <https://www.zamg.ac.at/cms/de/klima/informationsportal-klimawandel/daten-download/klimamittel> (accessed on 14 May 2021).
38. BFW. eBod—Digitale Bodenkarte von Österreich, 1 km-Raster. Available online: <https://bodenkarte.at/> (accessed on 17 May 2021).
39. Agrarmarkt Austria. INVEKOS Schläge Österreich 2020. Available online: <https://geometadateninspire.gv.at/metadateninspire/srv/eng/catalog.search#/metadata/e499eacb-df06-4a6a-8175-b9745eeeadc4> (accessed on 17 May 2021).
40. Statistik Austria. *Agrarstrukturhebung 2016: Schnellbericht 1.17*; Statistics Austria: Vienna, Austria, 2016; Available online: https://www.statistik.at/wcm/idc/idcplg?IdcService=GET_NATIVE_FILE&RevisionSelectionMethod=LatestReleased&dDocName=116146 (accessed on 17 May 2021).
41. ZAMG. Messdaten. Available online: <https://www.zamg.ac.at/cms/de/produkte/klima/daten-und-statistiken/messdaten> (accessed on 17 May 2021).
42. Krenn, A.; Winkelmeier, C.; Cattin, R.; Müller, S.; Truhetz, H.; Biberacher, M.; Eder, T. Austrian wind atlas and wind potential analysis. *DEWEK* **2010**. Available online: https://www.windatlas.at/downloads/20101117_Paper_Dewek.pdf (accessed on 15 September 2021).
43. Holmes, J.D.; Bekele, S. *Wind Loading of Structures*, 4th ed.; CRC Press: Boca Raton, FL, USA, 2021; ISBN 9780367273262.
44. ESA: Sentinel-2 User Handbook; European Space Agency: Paris, France, 2015. Available online: https://sentinel.esa.int/documents/247904/685211/Sentinel-2_User_Handbook (accessed on 15 September 2021).
45. R Core Team. *R: A Language and Environment for Statistical*; R Foundation for Statistical Computing: Vienna, Austria, 2020.
46. Ranghetti, L.; Boschetti, M.; Nutini, F.; Busetto, L. “sen2r”: An R toolbox for automatically downloading and preprocessing Sentinel-2 satellite data. *Comput. Geosci.* **2020**, *139*, 104473. [[CrossRef](#)]
47. Geoland. Orthofoto Offline Österreich. Available online: <https://www.data.gv.at/katalog/dataset/7cb3fb29-6b14-477b-a88b-a6a526b59b40> (accessed on 17 May 2021).
48. BEV. Digitales Oberflächenmodell. Available online: https://www.bev.gv.at/portal/page?_pageid=713,2875583&_dad=portal&_schema=PORTAL (accessed on 17 May 2021).

49. Geoland. Basemap.at Verwaltungskarte Raster Offline Österreich. Available online: <https://www.data.gv.at/katalog/dataset/703fce40-6116-4836-aca4-7dddc33912ab> (accessed on 17 May 2021).
50. BEV. Verwaltungsgrenzen (VGD). Available online: https://www.bev.gv.at/portal/page?_pageid=713,2601287&_dad=portal&_schema=PORTAL (accessed on 17 May 2021).
51. Minasny, B.; McBratney, A.B.; Wadoux, A.M.-C.; Akoeb, E.N.; Sabrina, T. Precocious 19th century soil carbon science. *Geoderma Reg.* **2020**, *22*, e00306. [[CrossRef](#)]
52. BMLFUW. Digitales Geländemodell 1 m: Niederösterreich. Available online: https://www.no.e.gv.at/noe/Karten-Geoinformationen/NOE_Geodaten_Angebot.html (accessed on 17 May 2021).
53. Zhu, C.; Fan, X.; Bai, Z. Spatiotemporal Pattern of Wind Erosion on Unprotected Topsoil Replacement Sites in Mainland China. *Sustainability* **2020**, *12*, 3237. [[CrossRef](#)]
54. Urban, T. *Wind Erosion in the Agricultural Landscape: The Wind Erosion Equation Used in GIS: Monograph*; Wydawnictwo Uniwersytetu Rolniczego: Kraków, Poland, 2013; ISBN 978-83-60633-97-7.
55. Skidmore, E.L.; Woodruff, N.P. Wind erosion forces in the United States and their use in predicting soil loss. In *Agriculture Handbook 346*; Agricultural Research Service, U.S. Dept. of Agriculture in cooperation with Kansas Agricultural Experiment Station: Beltsville, MD, USA, 1968; p. 44.
56. Moeys, J. Package “Soiltexture”. 2018. Available online: <https://cran.r-project.org/web/packages/soiltexture/soiltexture.pdf> (accessed on 15 September 2021).
57. Saleh, A.; Fryrear, D.W. Soil roughness for the revised wind erosion equation (RWEQ). *J. Soil Water Conserv.* **1999**, *54*, 473–476.
58. Zingg, A.W.; Woodruff, N.P. Calibration of a Portable Wind Tunnel for the Simple Determination of Roughness and Drag on Field Surfaces 1. *Agron. J.* **1951**, *43*, 191–193. [[CrossRef](#)]
59. Zikeli, S.; Gruber, S. Reduced Tillage and No-Till in Organic Farming Systems, Germany—Status Quo, Potentials and Challenges. *Agriculture* **2017**, *7*, 35. [[CrossRef](#)]
60. Mezősi, G.; Blanka, V.; Bata, T.; Kovács, F.; Meyer, B. Estimation of regional differences in wind erosion sensitivity in Hungary. *Nat. Hazards Earth Syst. Sci.* **2015**, *15*, 97–107. [[CrossRef](#)]
61. ESRI Environmental Systems Research Institute. *ArcGIS Pro*; ESRI: Redlands, CA, USA, 2020.
62. López, M.V.; de Dios Herrero, J.M.; Hevia, G.G.; Gracia, R.; Buschiazzi, D.E. Determination of the wind-erodible fraction of soils using different methodologies. *Geoderma* **2007**, *139*, 407–411. [[CrossRef](#)]
63. Shiyatyi, E.I. *Wind Structure and Velocity over a Rugged Soil Surface*; Vestnik Sel.-khoz. Nauki 10: Alma-Ata, Kazakhstan, 1965. (In Russian)
64. Jugder, D.; Gantsetseg, B.; Davaanyam, E.; Shinoda, M. Developing a soil erodibility map across Mongolia. *Nat Hazards* **2018**, *92*, 71–94. [[CrossRef](#)]
65. Tatarko, J. Soil Aggregation and Wind Erosion: Processes and Measurements. *Ann. Arid. Zone* **2001**, *40*, 251–263.
66. Morgan, R.P.C. *Soil Erosion and Conservation*, 3rd ed.; Blackwell: Malden, MA, USA, 2005; ISBN 978-1-405-11781-4.
67. Panagos, P.; Ballabio, C.; Poesen, J.; Lugato, E.; Scarpa, S.; Montanarella, L.; Borrelli, P. A Soil Erosion Indicator for Supporting Agricultural, Environmental and Climate Policies in the European Union. *Remote Sens.* **2020**, *12*, 1365. [[CrossRef](#)]
68. Zachar, D. *Soil Erosion*; Elsevier Scientific Pub. Co.: Amsterdam, The Netherlands, 1982; ISBN 9780080869773.
69. Strauss, P.; Schmaltz, E.; Krammer, K.; Zeiser, A.; Weinberger, C.; Dersch, G. *Bodenerosion in Österreich—Eine Nationale Berechnung mit Regionalen Daten und Lokaler Aussagekraft für ÖPUL: Endbericht*; The Federal Agency for Water Management: Petzenkirchen, Austria, 2020; Available online: <https://info.bmlrt.gv.at/dam/jcr:579b01e2-745e-4f38-83ce-1f3c87244380/Evaluierung%20%C3%96PUL%20und%20Bodenerosion.pdf> (accessed on 31 August 2021).
70. Panagos, P.; Borrelli, P.; Poesen, J.; Ballabio, C.; Lugato, E.; Meusburger, K.; Montanarella, L.; Alewell, C. The new assessment of soil loss by water erosion in Europe. *Environ. Sci. Policy* **2015**, *54*, 438–447. [[CrossRef](#)]
71. Frielinghaus, M.; Winnige, B.; Deumlich, D.; Funk, R.; Schmidt, W.; Thieme, J.; Völker, L. *Infomationsheft zum Landwirtschaftlichen Bodenschutz im Land Brandenburg: Teil Bodenerosion*; Landesamt für Verbraucherschutz und Landwirtschaft: Potsdam, Germany, 1999.
72. Jiang, L.; Xiao, Y.; Ouyang, Z.; Xu, W.; Zheng, H. Estimate of the wind erosion modules in Qinghai Province based on RWEQ model. *Res. Soil Water Conserv.* **2015**, *22*, 21–25. [[CrossRef](#)]
73. Cornelis, W.M.; Gabriels, D. Optimal windbreak design for wind-erosion control. *J. Arid Environ.* **2005**, *61*, 315–332. [[CrossRef](#)]
74. Weninger, T.; Scheper, S.; Lackóová, L.; Kitzler, B.; Gartner, K.; King, N.W.; Cornelis, W.M.; Strauss, P.; Michel, K. Ecosystem services of tree windbreaks in rural landscapes—A systematic review. *Environ. Res. Lett.* **2021**. [[CrossRef](#)]
75. Rezaei, M.; Sameni, A.; Fallah Shamsi, S.R.; Bartholomeus, H. Remote sensing of land use/cover changes and its effect on wind erosion potential in southern Iran. *PeerJ* **2016**, *4*, e1948. [[CrossRef](#)] [[PubMed](#)]
76. Sharma, A. Integrating terrain and vegetation indices for identifying potential soil erosion risk area. *Geo-Spat. Inf. Sci.* **2010**, *13*, 201–209. [[CrossRef](#)]
77. Woldemariam, G.; Iguala, A.; Tekalign, S.; Reddy, R. Spatial Modeling of Soil Erosion Risk and Its Implication for Conservation Planning: The Case of the Gobeles Watershed, East Hararghe Zone, Ethiopia. *Land* **2018**, *7*, 25. [[CrossRef](#)]
78. Verheijen, F.; Jones, R.; Rickson, R.J.; Smith, C.J. Tolerable versus actual soil erosion rates in Europe. *Earth-Sci. Rev.* **2009**, *94*, 23–38. [[CrossRef](#)]

-
79. Ellenberg, H.; Weber, H.E.; Düll, R.; Wirth, V.; Werner, W. *Zeigerwerte von Pflanzen in Mitteleuropa*, 3., Durchgesehene Auflage; Verlag Erich Goltze GmbH & Co. KG: Göttingen, Germany, 2001; ISBN 9783884525180.
 80. Böhner, J.; Schäfer, W.; Conrad, O.; Gross, J.; Ringeler, A. The WEELS model: Methods, results and limitations. *Catena* **2003**, *52*, 289–308. [[CrossRef](#)]